Motion of Sorbed Gases in Polymers

Wen-Yang Wen
Department of Chemistry, Clark University, Worcester, Massachusetts 01610 U.S.A.

1 Introduction

The mobility of sorbed gases in polymers is an interesting scientific problem with important technological implications. Considerable effort has been invested in understanding the sorption, diffusion, permeability, and selectivity of gases in polymers. The impetus for this work comes from applications such as polymer membranes for gas separation and polymer barriers for packaging.

Polymers can serve, in various forms, as barriers to protect inside matter from the outside environment. For example, they are used for food packaging, beverage bottling, and coating and casing for cables and electronic components. Polymers may be designed for applications requiring controlled penetrant sorption and transport such as dye penetration and binding in fibres and sheets containing absorptive fillers, as well as drug delivery systems for medical purposes.

The other important uses of polymers are in separations: gas separations, ultrafiltrations, and reverse osmotic applications. Membranes and hollow tubes are used to separate various components of gas mixtures: helium separated from natural gases, hydrogen recovered from industrial gases and coal gases, methane from carbon dioxide, oxygen from nitrogen. *etc.*

Before considering the interaction of gases and polymers, let us remember that there are various physical states for a polymer: crystalline state, glassy state, viscoelastic state, rubbery state, viscous-flow state, melted state, *etc.* Since most gases usually do not dissolve in crystals, the crystalline state of polymers will be excluded from our further consideration.

When the temperature of a glassy polymer is increased to its glass transition temperature, T_g, the polymer changes to the viscoelastic state with a significant decreases in its elastic modulus (see Figure 1). This change at T_g, is described as a free-volume limited relaxation attributed to the onset of segmental motions inside the polymer. Following a wide-spread usage among polymer chemists, we shall employ the word 'rubbers' to mean polymers at temperatures above T_g, which would include both 'viscoelastic' as well as 'rubbery' polymers.

Since polymers are usually saturated with air or other gases, they are evacuated to form gas-free samples. Let us consider what may take place when a gas-free film is exposed to a gas of pressure p at one side and to a vacuum at the other side.

First, the gas sorption (adsorption and absorption) will take place at the polymer surface. Next, the sorbed molecules will penetrate into the polymer matrix and begin the process of diffusion. After a certain period of time, the penetrant molecules will reach the other side of the polymer film, desorb at the surface, and evaporate into the vacuum as gas molecules. In this way the gas permeation process can take place through the polymer.

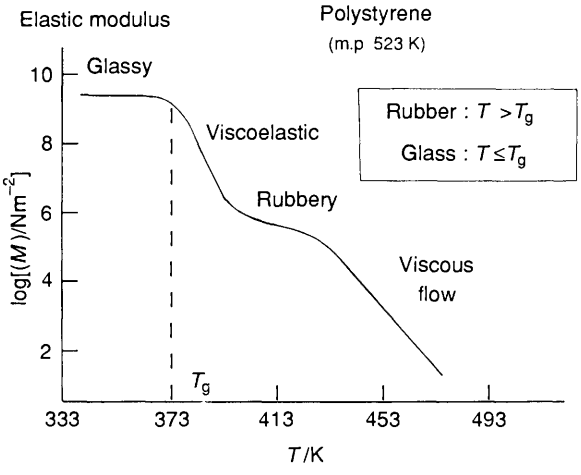

Figure 1 Plot of the elastic modulus of polystyrene *vs.* temperature.

In a steady-state permeation experiment, a gradient in the gas pressure is established and maintained across a polymer film. In this steady state, the constant flux J is measured on the low-pressure side of the permeation cell. The permeability $\tilde{P}$ is calculated from the equation.

$$J = \tilde{P} \cdot \Delta p / l \qquad (1)$$

where Δp is the pressure difference at the two sides of the film, and l is the film thickness. In a transient permeation experiment a sudden increase in the gas pressure is applied to one side of the film. We then measure as a function of time the amount Q_t of penetrant per unit film area that enters the low pressure side. At a certain time after the application of pressure, the steady state is reached and Q_t becomes proportional to time t. This time lag, θ, is given by

$$\lim_{t \to \infty} Q_t = J(t - \theta) \qquad (2)$$

as shown in Figure 2.

When gases are sorbed in polymers under constant pressure, the system is expected to reach a thermodynamic equilibrium without undue delay provided that the temperature is above the T_g of the polymer. On the other hand, the system is not expected to be in a true equilibrium state if the temperature is below the T_g of the polymer. The sorption and transport properties of gases in polymers can therefore be divided into two categories depending on whether the system temperatures are above or below T_g.

Penetrants may be sorbed gases, organic vapours, liquids, dyes, and other additives (sometimes called 'diluents'). In this review we shall confine our attention to penetrants which are gases under ordinary conditions.

Wen-Yang Wen obtained his B.S. degree from National Taiwan University in 1953 and his Ph.D. degree from the University of Pittsburgh in 1957. He did his postdoctoral research at Pittsburgh with Professor H. S. Frank and then at Northwestern University with Professor I. M. Klotz. In 1962 he joined the faculty of Clark University and has remained there since. His research interests include the structure of water and aqueous solutions, catalytic pyrolysis of coal and tar, and the dynamics of sorbed gas in polymers.

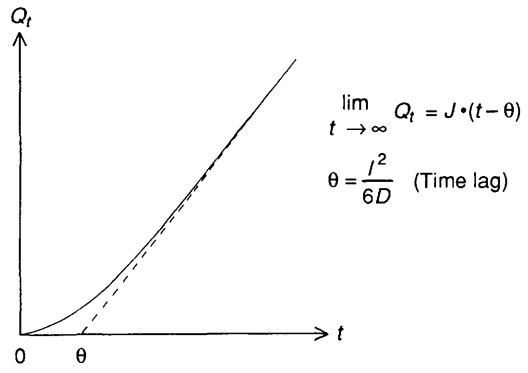

Figure 2 Amount Q_t of penetrant passing across unit area of a polymer film as a function of time t.

2 Macroscopic Observation

2.1 Gas Solubility in Polymers

As an example, Figure 3 shows sorption measurements for CO_2 in silicone rubber at 35 °C for pressure in the range of 1 to 54 atm.[1] The volume of the silicone rubber expands slightly with CO_2 sorption and this dilation has been determined and taken into account in their calculations. For pressure up to 20 atm, Henry's law seems to be obeyed, yielding the Henry's law constant, K_D, of 1.385 cm^3(STP)/(cm^3.polym.atm). At pressures greater than 20 atm, the c *vs.* p curve gradually deviates upward from Henry's law and the high solubility region can be described by a Flory–Huggin's treatment with an interaction parameter χ of 0.75.

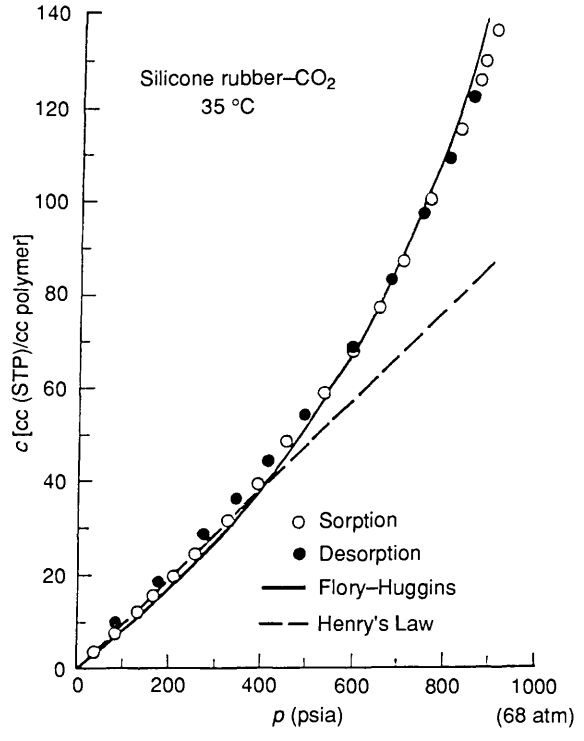

Figure 3 Sorption isotherms for sorption and desorption of carbon dioxide in silicone rubber at 35 °C.
(Reproduced by permission from *Macromolecules*, 1986, **19**, 2285.)

It is important to note that the solubility data determined by sorption and desorption experiments are the same. This is a distinct characteristic of the gas/rubbery-polymer systems indicating that the systems are in thermodynamic equilibrium. The T_g for the silicone rubber, poly(dimethyl siloxane), is − 123 °C and the temperature T of measurements for CO_2 is 35 °C, cledarly $T > T_g$.

Markedly different sorption–desorption response is observed for CO_2 in glassy polycarbonate (PC) at 35 °C as shown in Figure 4.[1] Since the T_g of PC is 150 °C, we have $T < T_g$ for this system. The desorption curve is distinctly different from the sorption curve, showing an effect of hysteresis. The solubility (c) of CO_2 is determined as a function of increasing pressure from about 2 to 60 atm, then the value of c is determined as a function of decreasing pressure from about 60 to 2 atm. The observed difference between the sorption and desorption curves is recognized as a characteristic of the gas/glassy-polymer system; it indicates that these systems are not in thermodynamic equilibrium.

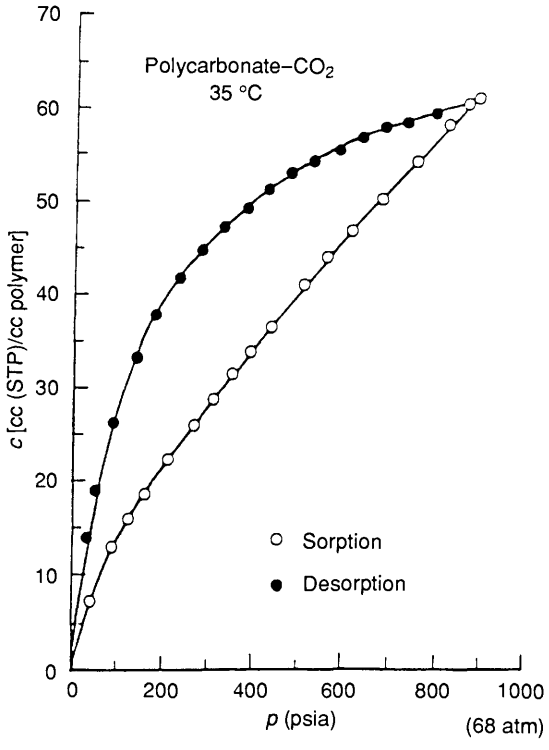

Figure 4 Sorption/desorption data illustrating the pronounced hysteretic response observed in the carbon dioxide/polycarbonate system at 35 °C.
(Reproduced by permission from *Macromolecules*, 1986, **19**, 2285.)

Figure 5 gives the results of Lowell and McCrum[2] for the solubility coefficient k plotted as a function of temperature for cyclopropane in linear polyethylene ($T > T_g$). The sharp increase in the values of k as the temperature climbs above the melting point T_m is attributed to the disappearance of the crystallites that existed in the linear polyethylene.

2.2 Gas Permeability

The gas permeability of a planar membrane is defined as

$$\bar{P} = J_s \cdot l / \Delta p$$

where J_s is the steady-state flux of the gas. The mean permeability $\bar{P}$ is the product of a mean diffusion coefficient $\bar{D}$ (a kinetic factor) and a solubility-related function $\bar{S}$ (a thermodynamic factor):

$$\bar{P} = \bar{D} \cdot \bar{S} \tag{3}$$

where

$$\bar{D} = \frac{1}{C_h - C_l} \int_{C_l}^{C_h} D(c)\mathrm{d}c \tag{4}$$

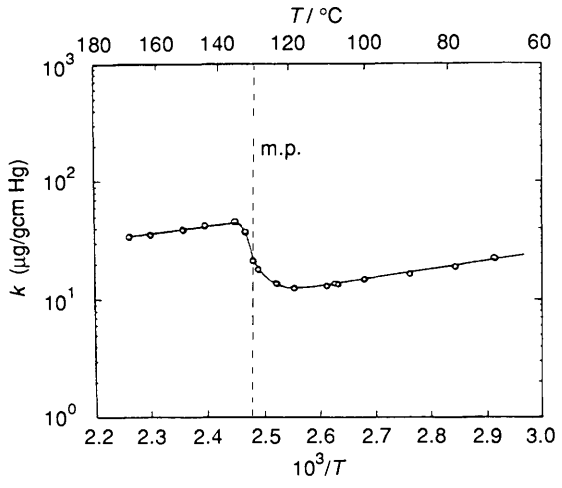

Figure 5 Temperature dependence of the solubility constant k for C_3H_6 in linear polyethylene above and below the melting point. Measurements taken at successively increasing temperature.
(Reproduced by permission from *J. Polym. Sci.: Part A-2*, 1971, **9**, 1935.)

$D(c)$ is the effective mutual diffusion coefficient and c is the local sorbed gas concentration in the membrane. C_h and C_l are the concentrations at the membrane interfaces when pressures p_h and p_l are maintained at these interfaces, respectively ($p_h > p_l$). The function $\bar{S}$ is defined by

$$\bar{S} = (C_h - C_l)/(p_h - p_l) = \Delta c/\Delta p \quad (5)$$

For example, the values of $\bar{P}$ for CO_2 are nearly constant and independent of pressure (for Δp in the range of 1 to 10 atm) across a membrane of rubbery poly(dimethyl siloxane), PDMS, at 35 °C ($T > T_g$);[3] in contrast, the permeability decreases appreciably with the initial increase of Δp across a membrane of glassy polycarbonate at 35 °C (T_g = 150 °C).[4]

2.3 Diffusion and Diffusion Coefficients

2.3.1 Fundamental Relations

Diffusion is the process by which the sorbed gas molecules are transported from one part of a polymer to another as a result of random motions of the molecules. The phenomenological theory of diffusion is based on the postulate that the flux of the penetrant is proportional to the concentration gradient measured perpendicular to the polymer film plane:

$$J = -D\partial c/\partial x \quad (6)$$

where D is the diffusion coefficient. By considering the mass balance of an element of polymer volume, it can be shown that the fundamental equation of diffusion takes the form of Fick's law given by

$$\partial c/\partial t = D\nabla^2 c \quad (7)$$

In many penetrant/polymer systems D depends, however, on the concentration. In this case, and also when the medium is not homogeneous so that D varies with the position (x,y,z), equation 7 becomes

$$\partial c/\partial t = \partial/\partial x(D\partial c/\partial x) + \partial/\partial y(D\partial c/\partial y) + \partial/\partial z(D\partial c/\partial z) \quad (8)$$

When diffusion takes place effectively in one direction along the x-axis only, equations 7 and 8 reduce, respectively to

$$\partial c/\partial t = D\partial^2 c/\partial x^2 \quad (9)$$

$$\partial c/\partial t = \partial/\partial x(D\partial c/\partial x) \quad (10)$$

The diffusion coefficient is a measure of the random molecular motions in that system. For example at 25 °C, the value of D for CO_2 in N_2 gas at 1 atm is 0.165 $cm^2\ s^{-1}$, but that in water is only 1.92×10^{-5} $cm^2\ s^{-1}$. In contrast, the diffusion coefficients of CO_2 at infinite dilution are 2.64×10^{-5} $cm^2\ s^{-1}$ in PDMS but only 1.2×10^{-8} $cm^2\ s^{-1}$ in polycarbonate glass at 35 °C.

The so-called 'apparent diffusion coefficient' may be calculated from the equation

$$D_a = l^2/6\theta \quad (11)$$

where θ is the observed time lag and l is the membrane thickness (see Figure 2). However, D_a does not have a simple meaning, since it is not directly related to a true molecular mobility. More often the effective diffusion coefficient $D(c)$ is determined for comparison with other techniques that probe molecular motion.

$D(c)$ in equation 4 can be determined from permeability and solubility measurements using the following relations:

$$D(c) = (\bar{P} + \Delta p(d\bar{P}/dp))(dp/dc)\Big|_{p = p_h} \quad (12)$$

$d\bar{P}/dp$ in the above expression is obtained from the pressure dependence of the mean permeability coefficient $\bar{P}$, and dp/dc is evaluated from the solubility–pressure relation. $D(c)$ is a function of the penetrant concentration and depends on the nature of the sorbed gas/polymer system and the temperature.

According to Stern's version[5] of Fujita's free volume theory,[6] the thermodynamic diffusion coefficient D_T is given by the expression,

$$D_T = RTA_d \exp(-B_d/\phi_a v_f) \quad (13)$$

where v_f is the fractional free volume, ϕ_a is the amorphous volume fraction of the polymer, and A_d and B_d are characteristic parameters. The meanings of these parameters are not clear but are thought to depend on the size and shape of the penetrant molecule. It should be noted that equation 13 may be applied to sorbed gases in rubbery polymers but not to penetrants in glassy polymers.

2.3.2 Some Experimental Observations

Diffusion coefficients at infinite dilution for five gases in polycarbonate are shown in Figure 6[8] as a function of kinetic diameter at 35 °C. The coefficients are derived on the basis of the dual-mode model with D_D and D_H referring to the diffusion coefficients for Henry's law species and Langmuir species, respectively (see Section 3.3.1).

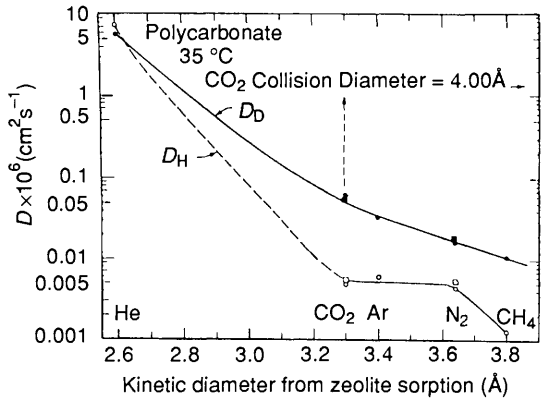

Figure 6 Diffusion coefficients for various gases in polycarbonate at 35 °C as a function of the kinetic diameter (molecular sieving dimension in zeolites). The solid points refer to the diffusion coefficients of the Henry's law species. The open points refer to the diffusion coefficients of the Langmuir species.
(Reproduced by permisison from *J. Membrane Sci.*, 1977, **2**, 165.)

The plot of infinite dilution coefficients D_0 *vs* the van der Waals volume is shown for a variety of penetrants in natural rubber and glassy poly(vinylchloride) in Figure 7 [9] In this figure, the effect on molecular mobility of penetrants is clearly contrasted for a rubber and for a glass In a rubber, as the kinetic diameter of the penetrant size approaches that of the normal hydrocarbons, C_nH_{2n+2} with $n = 3$, 4, or 5, the diffusivity reaches a plateau In the relatively rigid environment of the glassy polymer, the size and shape of penetrants are well discriminated resulting in a wide spread of their mobility

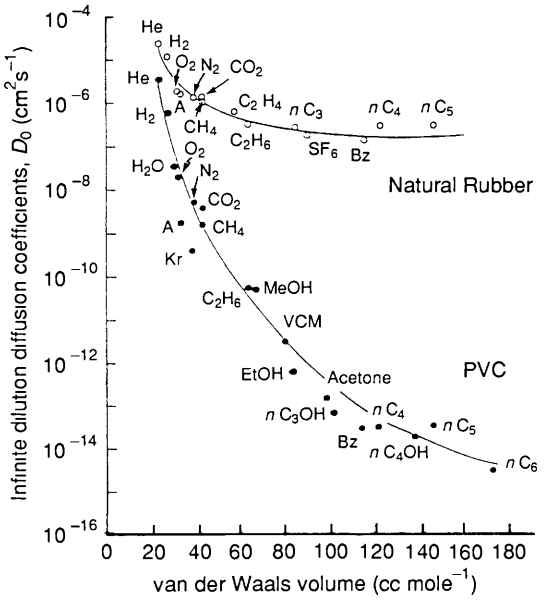

Figure 7 Diffusion coefficients for a variety of penetrants in natural rubber at 25 °C and rigid poly(vinyl chloride) at 30 °C plotted against the van der Waals volumes of the penetrants
(Reproduced by permission from 'Material Science of Synthetic Membranes', ACS Symposium Series, 1985, **269**, 28)

3 Theoretical Models

3.1 General Considerations

We may consider the solubility and motion dynamics of penetrants in polymers on various levels At the highest level we may wish to formulate a statistical mechanical description for the equilibrium and time-dependent properties of the whole system On this level the various effective potentials representing interactions among penetrant molecules and the polymer molecules are taken into account Thermodynamic equilibria may be considered to be established during the ordinary laboratory time scale for the penetrant/rubber systems but not for the penetrant/glass systems

At a second level, for the penetrant/glass systems, we may employ a lattice model for polymers and formulate stochastic rate equations for the penetrant motion The main charcteristic of this model is that the nearest-neighbour interactions between the molecules are treated properly and double occupancy of the lattice sites is excluded

At a third level for both glassy and rubbery polymers, the sorbed gas transport over large distances and long times may be modelled by macroscopic diffusion equations Transport properties such as diffusion coefficients and permeabilities are considered to reflect the average properties of the sorbed gas and polymer The widely used free-volume models may also be grouped to the third level of the description

3.2 The Pace–Datyner Theory of Diffusion

Pace and Datyner proposed a statistical mechanical model for diffusion of simple molecules in polymer [10] They assumed that (i) a polymer consists of bundles of parallel chains with coordination numbers four and that a small molecule can pass along the axis of the interchain space (or tube) with no activation energy In addition, they assumed that (ii) the penetrant molecule can move perpendicular to this axis by the bending separation of two polymer chains which will require activation energy The second type of motion is slow and determines the translational diffusion coefficients of the penetrant The chains are supposed to interact according to the DiBenedetto potential,[11] which asssumes the chain to be a sequence of Lennard–Jones centres (*e g* CH_2 units)

They derived lengthy expressions for the activation energy ΔE, diffusion coefficient D, and the frequency of chain openings ν that allow passage of penetrant molecules The expression for the diffusion coefficient contains a parameter that represents the mean-square jump length of the penetrant molecule

$$D = < L^2 > \nu/6 = D_0 \exp(-\Delta E/RT)$$

Jump lengths L, however, cannot be independently estimated by the theory and the values of L implied from experimental diffusion coefficients are too long (400—1000 Å) and physically unrealistic

Recently Kloczkowski and Mark[12] examined the Pace–Datyner theory in detail and suggested several improvements They obtained a lower activation energy and a lower jump length, but the values of L are still too high

3.3 Models for Gas/Glassy-polymer Systems

3 3 1 Models Assuming No Plasticization of Polymers

Mears[13] proposed a 'dual-mode' picture in which sorbed molecules can remain in one of two surroundings in the glassy polymer The first surrounding or 'mode' is that of the dissolved or mixed state, while the second mode is that of the trapped state, in which the sorbed molecules reside in defects (often called 'microvoids' or 'holes') that were frozen into the glass at the transition temperature T_g Various investigators demonstrated that gases show distinctly non-linear isotherms in glassy polymers and represented them as a sum of a Henry's law contribution (1st mode) and a Langmuir contribution (2nd mode)

$$C = C_D + C_H = k_D p + C'_H bp/(1 + bp) \quad (14)$$

where C is the total sorbed gas concentration, C_D is the concentration of dissolved molecules, C_H is the concentration of molecules trapped in holes, k_D is the Henry's law constant, C'_H is the concentration in the holes at saturation, b is the hole affinity constant, and p is the pressure of the penetrant in the gas phase

A dual-mode transport theory is introduced to augment the sorption theory Paul and Koros revised the transport theory to allow partial mobility of the trapped penetrant molecules [7] The total flux of penetrant in polymer glasses is given by

$$J = -D_D \nabla C - D_H \nabla C \quad (15)$$

where D_D and D_H are diffusion coefficients for the sorbed molecules in the dissolved and trapped modes, respectively In addition, the local equilibrium between the two modes are assumed to be established very rapidly These two modes are related by

$$C = C_D + C_H = C_D + KC_D/(1 + \alpha C_D) \quad (16)$$

where $K = C'_H b/k_D$ and $\alpha = b/k_D$ Combining equations 15 and 16 Paul and Koros derived the following expression for the flux

$$J = -D_D[1 + FK/(1 + \alpha C_D)^2)/(1 + K/(1 + \alpha C_D)^2)]\Delta C \quad (17)$$

where $F = D_H/D_D$ The time dependence of the penetrant concentration may be obtained by the combination of equation 17 and the continuity equation

$$\partial C/\partial t = -\nabla J \tag{18}$$

This transport model of Paul and Koros contains five parameters and can be used to fit the permeability and diffusion data The values of F obtained usually fall in the range of 0 04 to 0 6

One of the difficulties with the Paul–Koros model is that the flux equation (equation 15) does not contain terms that couple the two modes C_D and C_H The equation for the flux would contain terms that take into account the transport into and out of the holes Another difficulty with equation 15 is the implication that the hole domains are large enough to sustain diffusion

Frederickson and Helfand included the coupling terms which provide mobility to molecules that are trapped into holes [14] In addition to $C_D(x,t)$ and $C_H(x,t)$, the concentrations $C'_D(x)$ and $C'_H(x)$ are considered for the dissolved and trapped modes of sorption when they are fully saturated with the respective molecules Their derived expression for the total penetrant flux is

$$J = -\{[D_D^0 + KA - \alpha AC_H]\nabla C_D + [D_H^0 + A + \alpha AC_D]\nabla C_H\} \tag{19}$$

where

$$A = A_{HD}/\alpha \tag{20}$$

$$A_{KL} = (1/6)\int W_{KL}(y)y^2 dy \tag{21}$$

$$D_K^0 = A_{KK}C'_K \text{ for K, L = D or H} \tag{22}$$

α is a length that parameterizes the range of $W_{KL}(y)$ and D_K^0 is the diffusion coefficient for penetrant within the kth phase $W_{KL}(y)$ are phenomenological coefficients that reflect the rate at which penetrant molecules in mode L are transferred into a region of mode K a distance y away The authors noted the presence of the terms contained in equation 19 that couple the two modes C_D and C_H Furthermore they noted that the 'bare' diffusion coefficients D_D^0 and D_H^0 have been renormalized by KA and A, respectively The consequence of this is that even if penetrant molecules in the trapped mode have no intrinsic mobility ($D_H^0 = 0$), the exchange of molecules between modes provide mobility to trapped molecules This is definitely an improvement of the Paul–Koros expressions

With the assumption of the rapid local equilibrium equation 19 can be rewritten as

$$J = -D(C_D)\nabla C \tag{23}$$

where the effective concentration-dependent diffusion coefficient for the dissolved species is

$$D(C_D) = D_D^0 + 2KA/(1 + \alpha C_D) + KD_H^0/(1 + \alpha C_D)^2 \tag{24}$$

The permeability can now be calculated explicitly

$$\bar{P} = D_D^0 k_D[1 + 2KS(y_h - y_l)\cdot\ln(1 + y_h)/(1 + y_l) + KF/(1 + y_l)(1 + y_h)] \tag{25}$$

where $S = A/D_D^0$, $F = D_H^0/D_D^0$ and $y_l = bp_l$, $y_h = bp_h$ Equation 25 reduces to the Paul–Koros expression for the permeability in the special case of $S = 0$ and $P_l = 0$

In addition, Fredrickson and Helfand[14] treated the time lag and derived lengthy mathematical expressions, which are said to reduce to the result of Paul and Koros as a special limiting case Within the limitations of the case for non-swelling polymer glasses, their treatment seems to be quite satisfactory as a consistent dual-mode model for the penetrant transport

3 3 2 Models Which Consider Polymer Plasticization

The dual-mode model of Paul and Koros assumes, as does that of Fredrickson and Helfand, that the penetrant solubility in the polymer is sufficiently low so that the plasticizing (swelling) effects can be ignored However, such effects are measured and detected in a number of important physical applications Therefore, the dual-mode model of Paul and Koros was extended by Stern *et al* [15] to take into account the plasticization of the polymer by penetrants These investigators showed that the extended dual-mode model could be used to describe the solution and transport of methanol, benzene, and acetone in ethyl cellulose and of water in poly(acrylonitrile) as well as the solution of vinyl chloride in poly(vinyl chloride)

Recently Zhou and Stern[16] considered the effect of plasticization on diffusivity in the Henry's law mode and the Langmuir mode separately For convenience the authors assumed D_D and D_H to be exponential functions of C_D and C_H, respectively

$$D_D = D_D(0)\exp(\beta_D C_D) \tag{26}$$

$$D_H = D_H(0)\exp(\beta_H C_H) \tag{27}$$

where $D_D(0)$ and $D_H(0)$ are the mutual diffusion coefficients in the limits of infinite dilution β_D and β_H are empirical parameters that depend on the penetrant/polymer system and the temperature, and characterize the effects of plasticization on penetrant transport in the dissolved and trapped modes, respectively The effective diffusion coefficient D_{eff} is expressed by

$$D_{eff}/D(0) = \exp(\beta_D C_D)(1 + FK/(1 + \alpha C_D)^2)/(1 + K/(1 + \alpha C_D)^2) \tag{28}$$

where

$$F/F(0) = \exp[C_D(\beta_H K/(1 + \alpha C_D) - \beta_D)] \tag{29}$$

The ratio $D_{eff}/D(0)$ is plotted in Figure 8[16] in accordance with equation 28 as a function of the dimensionless penetrant pressure bp_h ($= \alpha C_D$) for the case with $p_l = 0$ As shown in the Figure 8, D_{eff} will increase with increasing plasticization ($\beta_D, \beta_H > 0$) and decrease as a result of antiplasticization ($\beta_D, \beta_H < 0$) or clustering of penetrant molecules Both effects can occur simultaneously, each effect predominating in a different pressure range This is illustrated for $\beta = -0\ 05$, for which the plot of $D_{eff}/D(0)$ passes through a maximum Such a maximum has been observed for water in poly(acrylonitrile)

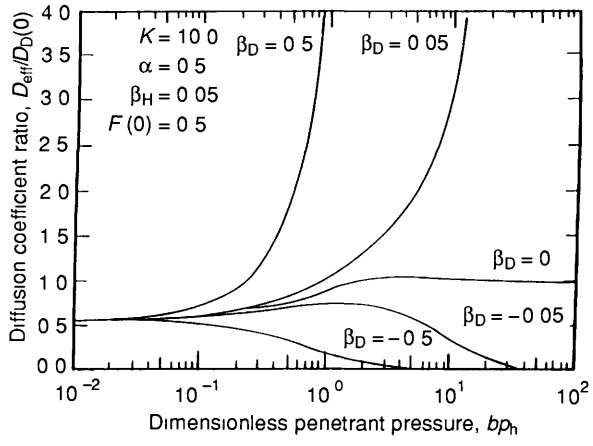

Figure 8 Ratio of diffusion coefficient $D_{eff}/D_D(0)$ as a function of dimensionless penetrant pressure bp_h for different values of β_D (Reproduced by permission from *J Polym Sci Part B Polym Phys*, 1989, **27**, 205)

This model of Stern and his co-workers[16] requires seven parameters $k_D, b, C'_H, D_D(0), D_H(0), \beta_D$, and β_H This substantial number of parameters, though it may be required by the complexity of the problem, can inhibit wide applications of this model

4 NMR Investigations

4.1 The Spin-Echo Method with a Pulsed Field Gradient for Diffusion

As a consequence of diffusion, the sorbed molecules change their locations in the polymer sample. In an inhomogeneous magnetic field, the component of the displacement in the direction of the field gradient changes the Larmor frequency of nuclear spins attached to the diffusing molecules. The amplitude of the spin echo is reduced as the molecules diffuse to greater distances during the interval τ between the pulses. The spin-echo method is based on the difference between the amplitude of the echo with and without a field gradient $G(= dH/dx)$ applied for a time δ. Although the main magnetic field ($H \approx 4$T) is changed only slightly by the gradient, which is typically about 0.02 T cm^{-1}, the high sensitivity of the NMR method can detect the changes of the Larmor frequency of nuclei moving more than about 10 nm.

With the pulse sequence shown in Figure 9,[17] the ratio R of spin-echo amplitude in the presence of a gradient A(G) to that with no gradient $A(0)$ is

$$R = A(\mathrm{G})/A(0) = \exp[-\gamma^2 D G^2 \delta^2 (\Delta - \delta/3)] \qquad (30)$$

Here γ is the gyromagnetic ratio of the nucleus and $\Delta \gg \delta$ is the diffusion time, *i.e.*, the interval between the times at which the consecutive gradient pulses are applied. The diffusion coefficient can be obtained from the slope of a plot of ln R *vs.* δ^2 at constant G and Δ.

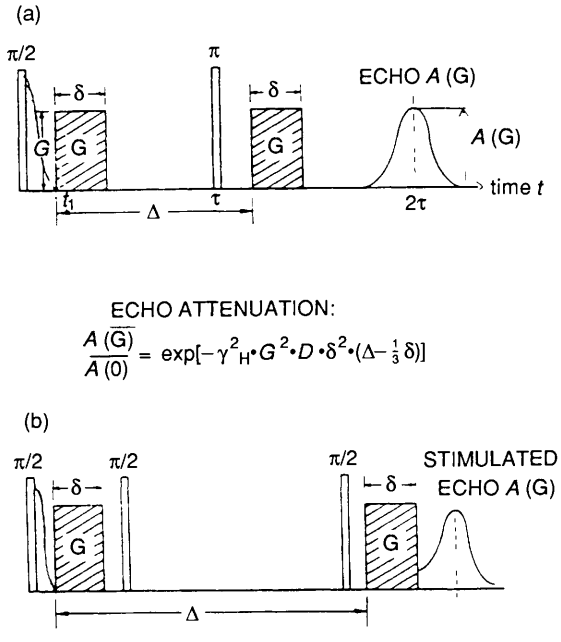

Figure 9 Pulsed-gradient spin-echo method (a) and pulsed-gradient stimulated-echo method (b) for the determination of the self-diffusion coefficient.
(Reproduced by permission from *J. Polym. Sci. Polym. Phys. Ed.*, 1985, **23**, 387.)

Zupancic *et al.*[17] studied the diffusion of sorbed butane in linear poly(ethylene) (PE) as a function of the vapour pressure of butane. The PE has a weight-average molecular weight of 52000 and a volume of crystallinity of 0.714. The observed pressure dependence of the diffusion coefficient is an exponential function of the vapour pressure p at 23 °C:

$$D = 3.77 \times 10^{-8} \exp(1.125p) \qquad (31)$$

where D is in the units of cm^2 s^{-1} and p is between 0.3 and 3 atm. Zupancic *et al.* did not report the temperature dependence of the diffusion coefficient.

4.2 Proton Spin-Lattice Relaxation Studies of Poly(dimethylsiloxane) under High Pressure of Gases by Assink

This molecular behaviour of PDMS exposed to gases pressurized up to 2040 atm was investigated by Assink.[18] Figure 10 shows the behaviour of proton T_1 as a function of pressure for the gases helium, nitrogen, and argon. At room temperature it is well above the temperature at which $(T_1)_{min}$ occurs, so that decreasing the molecular motion (bringing it closer to the resonance frequency) decreases T_1. Helium pressurization exhibits this typical pressure dependence of decreasing T_1 with increasing pressure. In contrast, a very small pressure dependence is exhibited by PDMS when nitrogen is used as the pressurizing medium, and the opposite pressure dependence is shown by PDMS when argon is used as the pressurizing medium.

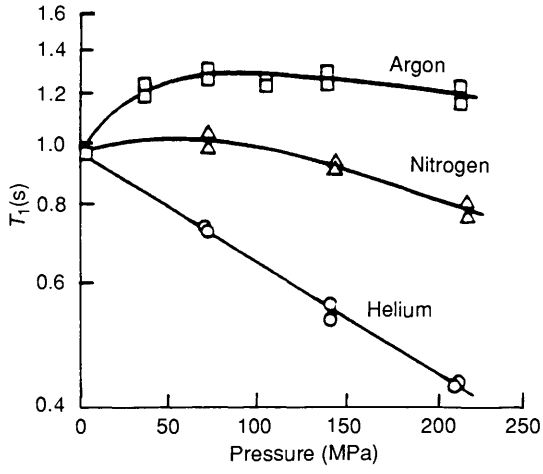

Figure 10 Spin-lattice relaxation time of PDMS *vs.* pressure for the gases helium, nitrogen, and argon.
(Reproduced by permission from *J. Polym. Sci. Polym. Phys. Ed.*, 1974, **12**, 2281.)

Before considering the mechanism involved we wish to examine the time behaviour of T_1 following the gas solution process. If a sample of PDMS is suddenly exposed to a soluble gas, its relaxation time should increase steadily from a small value to the equilibrium as the gas dissolves. It is known that the uptake of gas by the sample is proportional to $t^{\frac{1}{2}}$ for short times. If one assumes that the change of the rubber T_1 is directly related to the concentration of the sorbed gas, then one expects that it too should be proportional to $t^{\frac{1}{2}}$ as shown in Figure 11.

Due to its small atomic size and large solubility, helium gas applied to PDMS acts only as a pressurizing medium. In contrast two mechanisms are considered when nitrogen and argon gas pressures are applied to the polymer: they are pressurizing and plasticization mechanisms. The dissolved gas increases the internuclear distances of adjacent chains and decreases the effectiveness of their dipolar interaction, thus increasing the relaxation time T_1. This plasticizing effect of PDMS by argon is greater than that by nitrogen, as shown in Figure 10.

Figure 12[18] shows the proton T_1 of PDMS as a function of temperature and three gas pressures: at about 1 atm, under helium pressure of 1362 atm, and under argon pressure of 1362 atm. At atmospheric pressure, the motion which results in the T_1 minimum at − 73°C corresponds to the motion responsible for the glass transition temperature. But the T_g of PDMS is − 123 °C as measured by differential scanning calorimetry or dynamic mechanical spectroscopy. These techniques are sensitive to low freqencies ($\approx$ 1 Hz) while the frequencies that are characteristic of T_1 are near the Lamor frequency of the protons at 90 MHz. The temperature associated with the glass transition depends upon the frequency of the technique used to measure it. The glass transition temperature of − 73 °C by NMR T_1 method

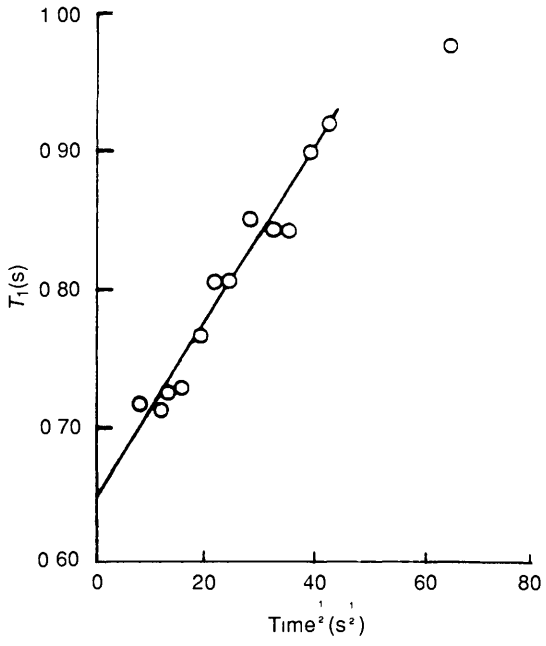

Figure 11 Spin-lattice relaxation time of PDMS exposed to 957 atm nitrogen at time zero
(Reproduced by permission from *J Polym Sci Polym Phys Ed*, 1974, **12**, 2281)

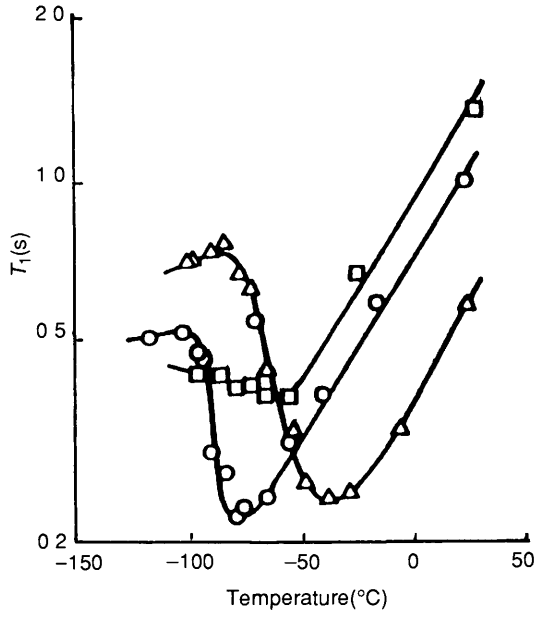

Figure 12 Spin-lattice relaxation time of PDMS *vs* temperature for various conditions, ○, helium at p = 1 atm, △, helium at p = 1362 atm, □, argon at p = 1362 atm
(Reproduced by permission from *J Polym Sci Polym Phys Ed*, 1974, **12**, 2281)

is 40 to 60 degrees above the T_g of − 123 °C by DSC or DMS methods The WLF equation can be used to correlate these temperature shifts with the frequency of observation

As discussed above we know that helium gas behaves as a pressurizing medium and decreases the molecular correlation frequency of the PDMS We expect, therefore, that the pressurization by argon is less distinct and is shifted to the left of the minimum for helium The minimum enables us to determine the temperature, − 61 °C, at which the molecular correlation frequency is near the resonance frequency The smaller shift of − 73 °C to − 61 °C must be interpreted as plasticization by the argon gas dissolving into the rubber and allowing motion at − 61 °C which would otherwise be allowed only at the higher temperature of − 35 °C

4.3 General Considerations of Relaxation Mechanisms and Motion of Gases Sorbed in Polymers

Let us consider carbon-13-enriched carbon dioxide As a pure gas, CO_2 may relax primarily by the spin–rotation (SR) mechanism through collisions When the gas is sorbed in a polymer, the contributions of various relaxation mechanisms are expected to change For example, simple liquids like CS_2 have approximately comparable relaxation contributions from the chemical shift antisotropy (CSA) mechanism through rotations and the SR mechanism through collisions [19]

Carbon dioxide dissolved in a polymer matrix is in a condensed phase and, therefore, should be closer to liquid CS_2 than gaseous CO_2 Although enriched CO_2 is used in the polymer experiments, homonuclear dipole–dipole (DD) relaxation is not likely since the sorbed gas is typically only several percent of the sample by weight when the gas pressure is about 10 atm (A good NMR signal in PC is obtained when the CO_2 pressure is at or above several atmospheres) However, heteronuclear DD relaxation between protons on the polymer and the carbon-13 of the CO_2 is highly probable since the protons have a significant concentration in the samples [20]

Each relaxation mechanism provides access to a different type of motional information Spin–rotation relaxation depends on collisional changes in the rotational angular momentum quantum number and would provide a measure of the collision frequency of the sorbed gas in the polymer The CSA mechanism depends on the rotational correlation time and thus provides information on molecular rotation The intermolecular dipole–dipole relaxation mechanism depends on the translational motion of the sorbed gas molecule through the polymer matrix and on the distance of closest approach to the polymer protons This mechanism provides a short-range measure of the translational diffusion coefficient of the penetrant molecule

The nature of the polymer matrix is also important in influencing the mobility of the penetrant Diffusion of penetrants through rubbers is expected to be characterized by a different formalism than diffusion through glasses Diffusion in rubbers may be treated as though the rubber is a simple liquid and the penetrant is dissolved in the polymer Molecular level information from spin relaxation can be used to test this approximation Penetrants in glassy polymers are usually described by the dual-mode model As discussed in Section 3 3, the penetrant in this model may be sorbed in either Langmuir sites or dissolved sites, the latter being comparable to the mode of sorption in a rubber Different translational diffusion times are assigned to the two types of penetrants in a glassy polymer From this viewpoint, one would expect changes in spin relaxation as one changes from a glassy polymer to a rubbery polymer or as one traverses the glass transition of a given polymer

A typical spectrum of CO_2 gas sorbed in thin strips of glassy polycarbonate (PC) is shown in Figure 13[20] along with a spectrum of the gas sorbed in powdered PC According to these spectra, the resonance frequencies for the $^{13}CO_2$ sorbed in powdered PC and in PC strips are rather different Since relaxation of gas sorbed in the bulk polymer is our primary interest, sufficiently thick samples (blocks or stacked disks) should be used so that a resolved resonance for the sorbed gas can be identified and measured

4.4 Relaxation Mechanisms for $^{13}CO_2$ in Silicone Rubber

In order to characterize various group motions in polymers, an increasing number of investigators are using a fractional correlation function of the type

$$\phi(t) = \exp[-(t/\tau_p)^{\alpha}] \qquad (32)$$

Cain *et al* also used this Williams–Watts type correlation

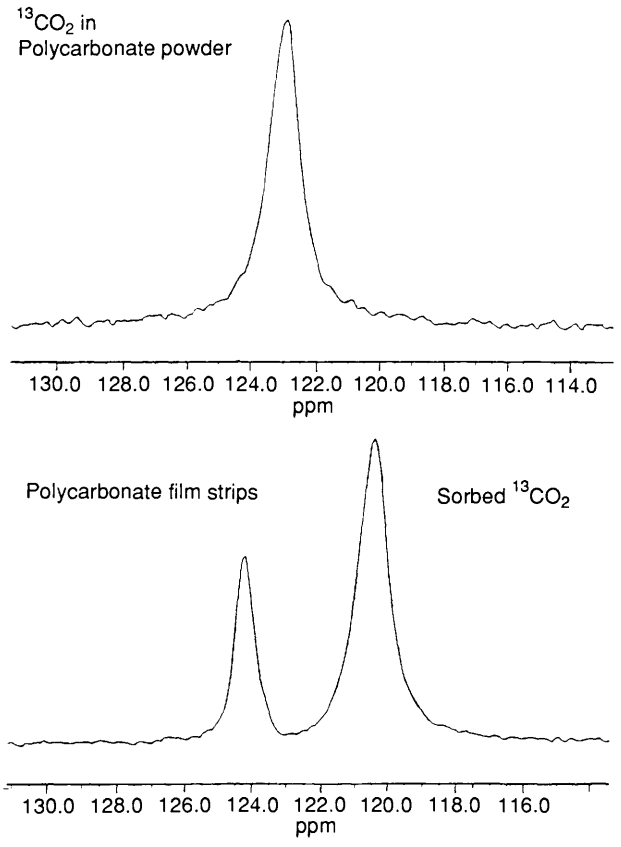

Figure 13 Carbon-13 NMR spectra of $^{13}CO_2$ dissolved in powdered polycarbonate and 5-mm polycarbonate strips. The free gas resonance is at 124.2 ppm. Both spectra recorded at 62.9 MHz. Note the relative amounts of dissolved and free carbon dioxide are not equivalent for these two samples.
(Reproduced by permission from *J. Phys. Chem.*, 1990, **94**, 2128.)

function to depict motions of CO_2 in silicone rubber.[21] In equation 32, τ_p is the central correlation time and sets the position of the distribution on the time axis. The parameter α, which falls in the range of $0 < \alpha < 1$, determines the width of the distribution.

The relaxation data modelling and fitting procedure begins with initial guesses for the values of six parameters: $\tau_{SR}(300\,K)$, the correlation time for spin rotation at 300 K; $\tau_{CSA}(300\,K)$, the correlation time for CSA at 300 K; b, the distance of the closest approach between a proton and a carbon-13 nucleus; ΔH, the activation energy; and α, the width parameter of the distribution. These parameter values are adjusted in an effort to fit the experimental data and minimize the sum of squares (the least squares). The parameters of the best fit are:

$$\tau_{SR}(300\,K) = 8.8 \times 10^{-14}\ s;\ \tau_{CSA}(300\,K) = 1.6 \times 10^{-13}\ s$$
$$\tau_{DD}(300\,K) = 3.8 \times 10^{-7}\ s;\ \Delta H = 1.6\ kJ\ mol^{-1} \quad (33)$$
$$b = 3.9 \times 10^{-8}\ cm;\ \alpha = 0.58$$

The average values for the dipole–dipole correlation time and translational diffusion coefficient are given by

$$\langle \tau_{DD} \rangle = \sum_k p_k \tau_k = 7.8 \times 10^{-7}\ s$$
$$\langle D_t \rangle = \sum_k p_k D_k = 1.8 \times 10^{-5}\ cm^2\ s^{-1} \quad (34)$$

where p_k is the weighting factor (or fractional population) for the kth relaxation time. Since $D_k = b^2/\tau_k$, the average diffusion constant corresponds to the harmonic average of the correlation time and *vice versa*.

It is interesting to note that the obtained average of the self diffusion coefficient, $1.8 \times 10^{-5}\ cm^2\ s^{-1}$, is close to the mutual diffusion coefficient of $2.64 \times 10^{-5}\ cm^2\ s^{-1}$ reported by Stern *et al.* from their permeability measurements of CO_2 sorbed in silicon rubber.[22] Given the complexity of the interpretation of the NMR data and the short-range viewpoint of the NMR experiment, the agreement is better than would be expected.

With regard to the spin rotation, the correlation time $\tau_{SR}(= 8.8 \times 10^{-14}\ s)$ found for $^{13}CO_2$ (10 atm) sorbed in silicone rubber turns out to be much closer to the value of the liquid CS_2 (9.3×10^{-14} s) than that for gaseous CO_2 (4.6×10^{-10} s).

As pointed out above, Stern *et al.* reported the diffusion coefficient of CO_2 in PDMS as $2.64 \times 10^{-5}\ cm^2\ s^{-1}$ at 35 °C.[22] According to Figure 14, however, the population fraction of CO_2 molecules having these high values of diffusion coefficients is very small. Then what is a qualitative explanation for this apparent discrepancy? The process of CO_2 permeation through the rubber under a pressure gradient may be imagined to take place in the following way.

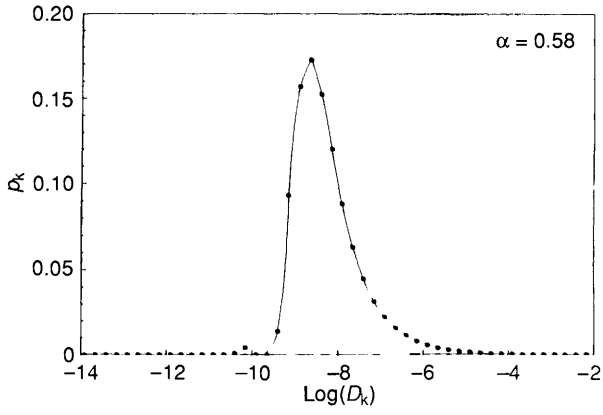

Figure 14 Population distribution of diffusion coefficients for $^{13}CO_2$ sorbed in silicone rubber.
(Reproduced by permission from *J. Polym. Sci.: Part B: Polym. Phys.*, 1990, **28**, 1737.)

The fractional population of CO_2 with diffusion coefficients of 10^{-6} to $10^{-4}\ cm^2\ s^{-1}$ is indeed very small, but this small population of CO_2 dominates transport. It is analogous to the important role played by the path of least resistance in a parallel circuit carrying a flowing current. The simple weighted averaging of diffusion coefficients in a system characterized by two or more diffusion coefficients leads to the parallel-circuit result. In relation to the sorbed gas diffusion problem at hand, the internal states would correspond to sites in the polymer matrix with different sorbed gas mobilities.

4.5 Relaxation Mechanisms of $^{13}CO_2$ in Polycarbonate Glass

For consideration of relaxation mechanisms for $^{13}CO_2$ in polycarbonate which is a glass at temperatures below 150 °C, a simple data set comparable to that for silicone rubber (Table 1) is shown in Table 2. Again a field dependence is apparent in the

Table 1 Relaxation times and nuclear Overhauser enhancement for $^{13}CO_2$ sorbed in silicone rubber at 273 K and 11 atm[20]

	Frequency/MHz			
	22.6	50.3	62.9	100
T_1/s	9.7		11.7	13.1
T_2/ms	150	150		
NOE	1.14		1.0	1.0

Table 2 Relaxation times and nuclear Overhauser enhancement for $^{13}CO_2$ sorbed in polycarbonate at 333 K and 5 atm[20]

	Frequency/MHz			
	22 6	50 3	62 9	126
T_1/s	4 6	3 6	3 3	2 2
T_2/ms	141	40		
NOE	1 28		1 08	1 0

T_1 data of Table 2, but one that is opposite to that of the silicone rubber system This type of field dependence is characteristic of CSA relaxation and specifically for the fast motion (short correlation time) regime A CSA contribution is an indication that rotational motion in this system must be slowed down relative to that in the silicone rubber This is not unreasonable considering that we have gone from the relatively high mobility of a rubbery matrix to that of a glass An NOE is also present in this system and, therefore, dipole–dipole relaxation must also be a contributor In addition, it is necessary to invoke a considerable contribution from spin–rotation relaxation

Cain *et al* [23] presented a quantitative interpretation based on a two-site, rapid exchange model In particular they follow the lattice model of Bendler, Shlesinger and Weiss [24] This model contains at least 13 potentially adjustable parameters $\tau_{SR}$and τ_{CSA} for the hole site, τ_{SR} and τ_{CSA} for the dissolved site, diffusion coefficients for hole-to-hole sites (D_{HH}), for hole-to-dissolved (D_{HD}), for dissolved-to-hole (D_{DH}), and for dissolved-to-dissolved (D_{DD}), distance of closest approach (b), activation energy for the hole site ΔH_H, activation energy for the dissolved site ΔH_D, the mole fraction of dissolved sites (X_D), and lastly the population of the dissolved site (P_D) as a function of temperature To obtain a credible interpretation, a number of these potential parameters are set to the literature values and a number of others are interrelated and thereby eliminated as adjustable (Eventually the number of adjustable parameters are reduced to five) This process does involve simplifying assumptions which may or may not be too severe

The parameters and the best-fit values obtained by Cain *et al* are listed below

$$\tau_{SR}(\text{dissolved}) < 1 \times 10^{-14}\ \text{s}$$

$$\tau_{CSA}(\text{dissolved}) = 4\,4 \times 10^{-11}\ \text{s}, \quad \tau_{CSA}(\text{hole}) = 4\,3 \times 10^{-8}\ \text{s}$$

$$\Delta H_D = 10\,5\ \text{kJ mol}^{-1} \quad D_{HH} = 1 \times 10^{-10}\ \text{cm}^2$$

A summary of constants entered into the fitting process may also be listed

$$D_{DD} = 1\,50 \times 10^{-7}\ \text{cm}^2\ \text{s}^{-1}, \quad \Delta H_H = \Delta H_D + 6\,2 = 16\,7\ \text{kJ mol}^{-1}$$

$$b = 3\,2 \times 10^{-8}\ \text{cm}, \quad X_H = 2 \times 10^{-3}(T_g - T) \qquad (35)$$

Overall, the interpretation of the spin relaxation data for $^{13}CO_2$ in glassy polycarbonate leads to a measure of local dynamics which is consistent with the conceptual basis of the dual-mode model Motion in the dissolved site is liquid-like and is similar to that observed in liquid CS_2 and not too different from CO_2 sorbed in silicone rubber Motion in the hole or Langmuir site is considerably slower, in agreement with the proposed nature of this site The lattice model provides a connection between the microscopic view of NMR data and the macroscopic measurement of translational mobility derived from permeability The dissolved-to-dissolved type of diffusion is the dominant contributor to permeability from the lattice model viewpoint The hole-to-hole diffusion was negligible, with a very small diffusion coefficient consistent with the assumption

The two-site model used here is consistent with the dual-mode picture and does provide a substantially better quantitative interpretation than a distribution of correlation times associated with a skewed bell-shaped curve Unfortunately, their data are not absolutely decisive in support of the dual-mode model It is the strong dependence of T_2 on temperature that could be matched by a two-site interpretation and could not be matched with the distribution model

5 Computer Simulation

Diffusion of small molecules in polymers may be simulated by computers using equilibrium or non-equilibrium molecular dynamics (MD) For example, an equilibrium MD simulation of an assembly of n-alkane-like chains together with a low concentration of one-centre Lennard–Jones particles has been performed by Trohalaki *et al* [25] This work is a logical extension of their work on n-alkanes without penetrants

The potential energy as a function of bond length is given by

$$E_b = (1/2)k_b(l - l_0)^2 \qquad (36)$$

where l_0 is the equilibrium bond length The deformation of the bond angle θ from its tetrahedral value θ_0 is governed by a potential function which is quadratic in $\cos\theta$,

$$E_\theta = (1/2)k_\theta(\cos\theta - \cos\theta_0)^2 \qquad (37)$$

The dihedral angle ϕ is constrained to lie mainly in the *trans* and *gauche* states by a torsional potential

$$E_\phi = k_\phi \sum_{n=0}^{5} a_n \cos^n\phi \qquad (38)$$

Non-bonded interactions are evaluated by a truncated Lennard–Jones potential

$$E_{LJ} = 4\epsilon^*[(r^*/r_{ij})^{12} - (r^*/r_{ij})^6] + c \quad \text{for } r_{ij} < 1\,5\,r^*$$
$$= 0 \quad \text{for } r_{ij} > 1\,5\,r^* \qquad (39)$$

The simulation consists of integration of Newton's equations of motion of the individual segments and penetrant particles In their work the parameters k_b, l_0, k_θ and so on were chosen such that the chain model will mimic a polyethylene molecule, and the segment represents a CH_2 group The simulation system consisted of a cubic box containing 500 CH_2 segments (25 chains) and four penetrant particles The simulations were performed at constant N, V, and E, with Δt of 10 fs A Cray Y-MP computer was employed and each simulation was run for 10^5 time steps for a duration of 1 ns

The self-diffusion coefficient of a component in a mixture, D_α (α = 1,2) can be calculated from the Einstein relation

$$D_\alpha = (1/6N_\alpha)\lim_{t\to\infty} \sum_{i=0}^{N_\alpha} < [\bar{v}_i(0) - \bar{v}_i(t)]^2 > \qquad (40)$$

where v_i is the velocity vector of a particle and N_α is the number of particles of type α Some of the results for self-diffusion coefficients are given in Table 3 for the case of a penetrant particle with r^* = 0 418 nm

The values of the diffusion coefficients found by simulation are somewhat higher, for example, for CO_2 at 361 K the simulation gives 17 8 × 10^{-5} cm^2 s^{-1}, while the experimental

Table 3 Self diffusion coefficients for polymer segment and penetrant with r^* = 0 418 nm[25]

T/K	D(polymer)/10^{-5} cm^2 s^{-1}	D(penetrant)/10^{-5} cm^2 s^{-1}
421	7 082 ± 0 462	28 23 ± 2 57
361	6 013 ± 0 208	17 81 ± 0 54
300	3 848 ± 0 431	13 38 ± 0 93
240	1 556 ± 0 112	7 16 ± 0 31

value is 4 44 × 10^{-5} cm^2 s^{-1} The major factor most likely to have given rise to these discrepancies is the difference in liquid density At 361 K the simulated system has a density of 0 576 g cm^{-3}, whereas the experimental C_{20} system has a density of about 0 741 g cm^{-3} at 13 6 atm The much larger free volume available in the simulated system is considered by Trohalaki *et al* to be responsible for the increased diffusion coefficients

Gusev and Suter[26] have presented a theory for the solubility of small particles in static structures of host matrices This theory is based on the statistics describing a gas dissolved in a polymer with sites that can be occupied by, at most, one solute particle (a spatial Fermi gas) The theory has been applied to the methane solubility in computed matrices of amorphous polycarbonate that cannot be plasticized The theory seems to yield the correct order of magnitude and the proper functional form of the sorption isotherm The computed distribution functions

$$\rho(p,1/b) = [1/c(p)]dc/d(1/b) \quad (41)$$

for the methane solubility in the glassy polycarbonate indicate that the sites with the values of $1/b \approx 10$ bar are of special importance, in agreement with the dual-mode sorption model with $b_H = 0\ 095\ bar^{-1}$ However, according to the authors, the distribution of sites is of a form that does not render it amenable to a quantitative reduction to the shape predicted by the dual-mode model One may speculate tentatively either that there is only one very broad distribution of sites or that the distribution of the Langmuir mode is narrow while the distribution of the Henry's law mode is broad

6 Conclusions

Various workers have investigated gas sorption and transport for many years, mostly from macroscopic viewpoints The time has come for researchers to characterize the motions of the sorbed gas in polymers on the molecular level The dual-mode model, which has been employed by a large number of polymer chemists and engineers, is now under scrutiny by some investigators Early results of a few NMR experiments and computer simulations are beginning to shed new light on the motional dynamics of both the penetrants and polymer chains The jury is still out and the outcome for the verdict on the dual-mode model is yet uncertain, but the time for its unravelling cannot be too far away

Acknowledgements The author wishes to acknowledge grant supports from the NSF (# DMR-9001678) and the Department of the Army (# DAAL03-91-G-0207) His principal co-investigators are Alan A Jones and Paul T Inglefield

7 References

1 G K Fleming and W J Koros, *Macromolecules*, 1986, **19**, 2285
2 P N Lowell and N G McCrum, *J Polym Sci Part A-2*, 1971, **9**, 1935
3 S A Stern, V M Shah, and B J Hardy, *J Polym Sci Part B Polym Phys*, 1987, **25**, 1263
4 T A Barbari, W J Koros, and D R Paul, *J Polym Sci Part B Polym Phys*, 1988, **26**, 709
5 S S Kulkarni and S A Stern, *J Polym Sci Polym Phys Ed*, 1983, **21**, 441 and 467
6 H Fujita, *Fortschr Hochpolym Forsch*, 1961, **3**, 1
7 W J Koros, D R Paul, and A A Rocha, *J Polym Sci Polym Phys Ed*, 1976, **14**, 687
8 W J Koros, A H Chan, and D R Paul, *J Membrane Sci*, 1977, **3**, 165
9 R T Chern, W J Koros, H B Hopfenberg, and V T Stannett, *ACS Symp Ser*, 1985, **269**, 28
10 R J Pace and A Datyner, *J Polym Sci Polym Phys Ed*, 1979, **17**, 437, 453, and 465
11 A T DiBenedetto, *J Polym Sci*, 1963, **A-1**, 3459
12 A Kloczkowski and J E Mark, *J Polym Sci Part B Polym Phys*, 1989, **27**, 1663
13 P Meares, *J Am Chem Soc*, 1954, **76**, 3415
14 G H Fredrickson and E Helfand, *Macromolecules*, 1985, **18**, 2201
15 S A Stern and V Saxena, *J Membrane Sci*, 1980, **7**, 47, 1982, **12**, 6
16 S Zhou and S A Stern, *J Polym Sci Part B Polym Phys*, 1989, **27**, 205
17 I Zupancic, G Lahajnar, R Blinc, D H Reneker, and A Peterlin, *J Polym Sci Polym Phys Ed*, 1978, **16**, 1399
18 R A Assink, *J Polym Sci Polym Phys Ed*, 1974, **12**, 2281
19 H W Spiess, D Schweitzer, U Haberlen, and K H Hausser, *J Magn Res*, 1971, **5**, 101
20 E J Cain, W -Y Wen, R D Jost, X Liu, Z P Dong, A A Jones, and P T Inglefield, *J Phys Chem*, 1990, **94**, 2128
21 E J Cain, A A Jones, P T Inglefield, R D Jost, X Liu, and W -Y Wen, *J Polym Sci Part B Polym Phys*, 1990, **28**, 1737
22 S A Stern, V M Shah, and B J Hardy, *J Polym Sci Part B Polym Phys*, 1987, **25**, 1263
23 E J Cain, W -Y Wen, A A Jones, P T Inglefield, B J Cauley, and J T Bendler, *J Polym Sci Part B Polym Phys*, 1991, **29**, 1009
24 J T Bendler, M F Shlesinger, and G H Weiss, *Macromolecules*, to be submitted
25 S Trohalaki, A Kloczkowski J E Mark, D Rigby, and R J Roe, in 'Computer Simulation of Polymers', ed R J Roe, Prentice Hall, 1991, pp 220–232
26 A A Gusev and U W Suter, *Phys Rev A*, 1991, **43**, 6488